FLIGHT TEST RESULTS FOR PERFORMANCE-BASED ICE DETECTION

Christoph Deiler[1]

[1]DLR – German Aerospace Center, Institute of Flight Systems, 38108, Braunschweig, Germany

Abstract

Supercooled large droplets (SLD) icing conditions have been the cause of severe aircraft accidents over the last decades. Existing countermeasures, even on modern airplanes, are not necessarily effective against the resulting ice formations, which raises a demand for reliable detection of SLD conditions for safe operations. New ice detection approaches and innovative sensor hybridization targeting a fast and reliable SLD-ice detection are the core of the EU funded Horizon 2020 project SENS4ICE. The performance-based (indirect) ice detection methodology is key to this hybrid detection approach and based on the changes of airplane flight characteristics under icing influence. The paper provides an overview on the indirect ice detection (IID) algorithm developed in SENS4ICE together with some exemplary results from both SENS4ICE flight test campaigns in North America (USA, February/March 2023) and Europe (France, April 2023).

Keywords: aircraft icing; aircraft flight performance; ice detection; flight test data evaluation

1. Introduction

Icing can have hazardous effects on airplane performance characteristics and can be a limiting factor for the safe flight envelope. The change of the dynamic behavior and potential premature stall raise the need for pilot situational awareness and an adaption of control strategy. Different accidents worldwide have shown the criticality of icing related aircraft characteristics degradations, e.g., Refs. [1, 2, 3, 4], especially when caused by supercooled large water droplets (SLD). Although in most cases the involved aircraft were equipped with state-of-the-art ice protection systems, the hazardous effects of SLD ice accretion often led to catastrophic events. These icing conditions can pose a high risk to the aircraft, crew and passengers, which requires specific detection and countermeasures to assure aircraft safety during flight. The certification of (modern) transport aircraft for flight into (known) icing conditions was mainly based on the certification requirements given in the so-called App. C to e.g., CS-25. But with the identified hazard to fixed-wing aircraft resulting from SLD, the certification requirements were extended by the new App. O including SLD ice in 2014. From now on, manufacturers must prove that a newly developed airplane is also safe for flight into the even more hazardous SLD icing conditions. For flight safety it is now mandatory to detect the presence of SLD icing early. Furthermore, monitoring the aircraft's remaining capabilities during prolonged flight in icing conditions would give relevant information to the pilots about the required adaption of operation, e.g., urgent need to enter air masses with sufficiently warm temperatures to melt ice accretions on the airframe if the aerodynamics are significantly degraded. As a complicating fact, predicting the distinct change of aircraft characteristics caused by SLD ice formation is challenging and still topic of current aviation research.

Most of the existing ice protection systems (IPS) on transport aircraft require a significant amount of energy provided on board. Thermal ice protection systems of mainly commercial aircraft usually rely on bleed air, which reduces the engine effectiveness and increases fuel consumption. Using such a system preventively therefore has a direct impact on aircraft emissions and operation cost. A more deliberate activation of the IPS can lead to more efficient but safe flight operations for which a reliable information about, e.g., the IPS effectiveness against the current icing encounter would

Figure 1 – Embraer Phenom 300 flight test bench: prototype aircraft with all modification for the SENS4ICE North America flight test campaign; credit Embraer.

be necessary. This information could be provided by suitable ice detection methods giving a hint about the presence of icing conditions, actual ice formation on the airframe and the effect on the flight characteristics [5, 6]. Moreover, it would also open possibilities for the modification of existing systems by modulating the thermal power according to the current need, directly reducing the energy consumption and increasing the aircraft efficiency.
The goal of the European Union Horizon 2020 Project "'SENSors and certifiable hybrid architectures for safer aviation in ICing Environment"' (SENS4ICE) project is to provide a more comprehensive overview on the icing conditions, ice formation and aircraft degradation status including the aircraft's remaining capabilities (icing-related change in aircraft flight physics, i.e., degraded aircraft performance) [7, 8]. Within SENS4ICE the "indirect ice detection" (IID) was further developed and matured and is one important project pillar [6]. It is a novel methodology and system for the on-board surveillance of aircraft flight performance used for ice detection purposes and was originally formulated and presented as a performance-based ice detection methodology, e.g., in Ref. [5], being already under patent protection in several countries [9]. It utilizes the effect of aircraft performance degradation due to ice accretion on the airframe resulting in a change of aerodynamics. The idea of the IID is not restricted to an application on large transport aircraft, but can also enable a reliable ice detection for aircraft systems, such as small UAV, which currently have no ice detection or protection system but operate in hazardous environments with very different icing conditions. The SENS4ICE project contained two major icing flight test campaigns: the North America campaign using an Embraer Phenom 300 prototype aircraft (see Fig. 1) and the European campaign with an ATR 42-320 (see Fig. 2) operated by Safire [8, 10]. This paper contains first evaluation results from the North America fight test campaign conducted between February 22nd and March 10th, 2023, out of St. Louis Regional Airport (Alton, IL, USA) and the European fight test campaign conducted in April 2023 out of Toulouse (France) with a focus on the IID ability to reliably detect the performance degradation caused by different icing during several example ice events.
This paper is structured as follows:

- the SENS4ICE approach for a more comprehensive view on the aircraft icing situation to enhance flight safety is presented in section 2;
- a brief description of the indirect ice detection methodology based on the observed aircraft flight performance variation and the specific implementation of the detection algorithm for the SENS4ICE purpose are given in section 3;
- exemplary flight test data analysis from SENS4ICE icing flight test campaigns reflecting the system performance with regard to the ability of reliable ice detection in section 4 and section 5.

Finally, a summary with initial conclusions are given in section 6.

Figure 2 – Safire ATR 42-320 flight test bench (MSN 78): aircraft with all modification for the SENS4ICE European flight test campaign at Toulouse/Francazal airport; credit DLR/Safire.

2. A Comprehensive View on Aircraft Icing Situation: The SENS4ICE Approach

Since the 1990s, accident analysis revealed the criticality of SLD-icing events for aviation safety, which forces the regulators to issue new certification requirements, e.g. in the App. O to CS-25 (EASA) or FAR Part 25 (FAA). But for certain aircraft types - mainly related to their size, design and operational profile - icing caused by smaller drops can also degrade the flight characteristics if the conditions encountered are characterized by a large water content leading to large and fast accumulation of ice on the aircraft, classified as severe icing. Hence, although the atmospheric icing conditions cause different ice accumulation on the airframe, the major risk for aviation safety is the aerodynamic degradation, which is only dependent on the size and location of ice accumulation and not specifically the conditions causing these. In addition, also the severity in terms of e.g., ice accumulation rate, is not a comprehensive indication of the real risk to the ongoing aircraft operation, if ice is only forming on unprotected surfaces not causing a significant degradation. Anyway, merging all the information available gives the most comprehensive view on the current icing situation, the aircraft condition and remaining safe operational capabilities. This is one main focus of the SENS4ICE detection approach to hybridize the sensing and support pilots to make a decision on the flight procedures required for the current icing situation and the dealing with supercooled large droplets in particular.

In a layered approach, a hybrid ice detection system (HIDS) is forming the core function accompanied by additional new nowcasting and enhanced weather forecasting. The latter allows to initially prevent the flight through hazardous icing conditions from a strategic and tactical point of view, whereas the hybrid detection architecture provides the necessary information to the flight crew for the IPS activation and the execution of safe exit strategies, when required. It combines in-situ measurement from various ice detection sensor technologies based on different physical principles (optical or remote sensing and ice accretion detection) with an indirect detection methodology. Hence, the HIDS gives a more general overview on the current aircraft icing than an individual system alone. In addition, the indirect detection methodology monitoring the current aircraft flight characteristic reveals the degraded aircraft flight envelope, which is essential for loss of control prevention. An overview on the layered safety concept is given in Fig. 3. The concept targets a general application and safety enhancement for fixed-wing aircraft icing and is not only dedicated to aircraft already certified for flight into known icing conditions (App. C). It intentionally goes beyond current certified aircraft systems proving safe operations in icing conditions.

The inner layer of the SENS4ICE safety concept in Fig. 3 focuses on the detection of the (remaining) safe flight envelope. This is at first independent of the icing conditions and includes a prediction of the current aircraft flight performance compromised by ice accretion which is directly related to the aerodynamic degradation. It is assumed that for safe flight operations an information about the current flight performance and aerodynamic degradation is more beneficial than a sole direct detection of potential icing conditions in flight without any further interpretation. The latter only allows to conclude on the need to leave the conditions or the ability to maintain but does not support the pilots in any other way during the further operation. Hence, the SENS4ICE hybridization combines the two different but complementary approaches of direct sensing – atmospheric icing conditions and ice ac-

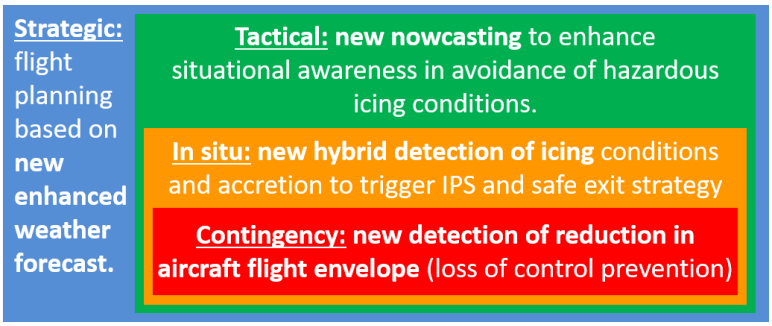

Figure 3 – SENS4ICE layered safety concept

cretion on specific surfaces – and indirect ice detection through predicting the degraded aircraft flight characteristics. There are several potential aircraft icing states which are not indicated correctly by a sole system. For example, when the aircraft enters icing conditions, accretion sensors and the IID do not directly indicate ice formation or a performance loss, whereas sensors monitoring the surrounding air will give a first indication of icing. But when the aircraft has ice on the airframe and leaves the icing conditions, the atmospheric sensor technologies will not give an indication whereas accretion based sensors or the IID might correctly announce icing. Furthermore, when the ice is also removed from the accretion sensor surface, there might still be some ice formation present on the airframe (protected and/or unprotected surface), which will then only be indicated by the IID if the aerodynamic degradation is significant. Hence, this simple example shows why the SENS4ICE hybrid approach might be key to safe aircraft operation in a wider icing envelope.
For safe aircraft operation in icing conditions, the most relevant question is about the potential degradation of aerodynamics in the presence of ice accretion. If icing is present and also correctly announced by direct sensors, the flight performance and aircraft characteristics might not be degraded. Hence, if ice formation on the airframe has no adverse effects and pilots are aware of the situation, there is no need to take any actions to maintain safe operations. These would only be required if a degrading effect on aerodynamics is detected. With this envelope expansion, operations in icing conditions could be enhanced and there is a potential for certification in a wider range of icing conditions.

3. Airframe Ice Detection through Flight Performance Monitoring

One major effect of aircraft ice accretion is a significant drag increase due to surface roughness changes, parasitic influence of ice formations and local flow separation. Another effect of icing is a change of the aircraft lift behavior, causing e.g., earlier or more abrupt flow detachment with increasing angle of attack and/or a reduction in aircraft lift slope. Both together significantly alter the aircraft flight performance, which can be monitored during flight. Figure 4 illustrates the typical icing-induced change of the lift and drag curves as generally described, e.g., in the AGARD report 344 [11]. Icing will also change the aircraft's flight dynamics (e.g., pitching and rolling moment), but these are not as specific as the general impact on lift and drag. Furthermore, the control characteristics are negatively affected by icing and change the aircraft behavior differently according to the specific occurrence of ice accretion. As these changes are very difficult to detect during flight, the IID relies on the icing related change of aircraft flight performance [5, 6].
Aircraft flight performance monitoring can provide crucial information to the pilots about the current (limited/degraded) aircraft capabilities while only requiring the sensor information already available on all modern airliners and business jets. The advantage of the developed methodology is that it relies only on the change in flight performance (i.e., steady flight states) contrary to the many failed attempts (e.g., in Refs. [12, 13, 14, 15, 16, 17]) based on the estimation of changes in the aircraft's dynamic behavior or a combination of both. The change/degradation in the flight performance is an indicator of ice accretion that is both robust and available throughout the whole flight: unlike the approaches based on the detection of changes in the aircraft dynamical behavior, it can also be used during steady flight conditions (majority of a normal operational flight) and can detect icing effects significantly before entering into stall. It is important to highlight that the method within the IID is

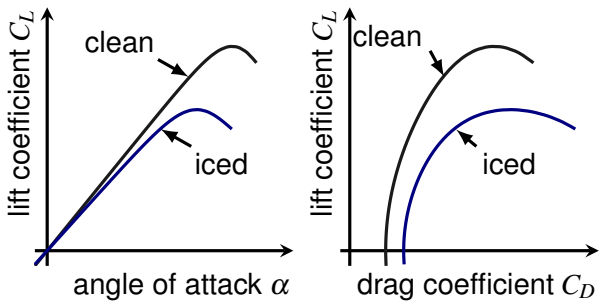

Figure 4 – Expected icing influence on aircraft lift and drag coefficient; adapted from [11]

focused on the flight performance changes with no need of any additional dynamic aircraft excitation. Such an excitation is not acceptable during normal operations as stated in Ref. [14] and especially not when flying with an aircraft that has a reduced (unknown) critical angle of attack due to icing.
The basic assumption for the indirect ice detection using performance monitoring is the possibility to distinguish between (very slow and small) performance variation of a single aircraft over lifetime in service (or within a fleet of same type) and the (much faster) performance variation caused by icing. Factors causing the flight performance variations across airplanes from the same type are, for example, production tolerances, aircraft skin repairs, aircraft skin contamination (e.g., dirt), engine aging causing reduced efficiency, or engine contamination. The aircraft flight performance can be seen as follows:

$$\begin{aligned} \textbf{Flight Performance} = \ & \text{Nominal Aircraft Performance} \\ & + \text{Expectable Variation} \\ & + \textit{Variation to be detected} \end{aligned}$$

whereby the "Expectable Variation" part gathers the effects mentioned previously and the "*Variation to be detected*" is subject to the indirect (performance-based) ice detection approach. The first step is to determine the typical and most extreme flight performance variation ("Expectable Variation") encountered during regular airline operations (due to a real performance variation or sensor errors). This was done in a basic evaluation of airline operational flight data in Refs. [5, 18] to initially verify the feasibility of the approach. For the SENS4ICE flight test benches, similar analysis had been conducted on less data but with more "in-sight" knowledge about the aircraft types due to the involvement of the manufacturers in the IID development. The results of this analysis are given in Refs.[19, 20, 21, 22] for both flight test platforms. The measured performance variation of each aircraft indicated that the average variation in normal flight is below the expected influence of airframe ice accretion on flight performance (using the available test data). It can furthermore be reliably assumed that the variation above the 90% quantile (of data analyzed) results from the external influence which can be ignored for the ice detection and circumvented (e.g., for large scale atmospheric disturbances or dynamic maneuvers) or filtered (e.g., for measurement noise) within the designed algorithm. This was the successful first step for the further IID development within SENS4ICE.
The basic idea of the performance-based ice detection method is to compare the current (possibly ice-influenced) aircraft flight performance characteristics with a known reference (see Fig. 5). The

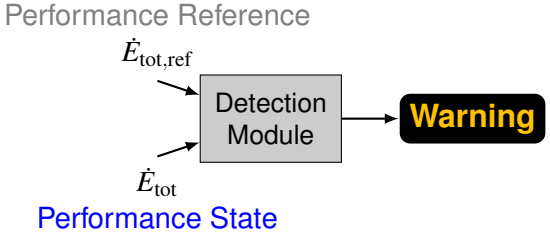

Figure 5 – Basic principle of the IID method based on the aircraft power imbalance; from [5]

flight performance can be defined as a power imbalance (change of total energy) $\dot{E}_{tot}$ for the current state and the reference, which allows representing the change of aircraft characteristics in a single parameter. Consequently, this reduces the complexity of the detection algorithm. It further combines the individual parts of the aircraft performance related to aerodynamics and engines in a single observation. The power imbalance $\dot{E}_{tot}$ can be formulated as

$$\dot{E}_{\mathrm{tot}} = V_{\mathrm{TAS}} \cdot \dot{V}_{\mathrm{TAS}} \cdot m_{\mathrm{AC}} + \frac{1}{2} \cdot V_{\mathrm{TAS}}^2 \cdot \dot{m}_{\mathrm{AC}} + g \cdot \dot{H} \cdot m_{\mathrm{AC}} + g \cdot H \cdot \dot{m}_{\mathrm{AC}} \ , \tag{1}$$

with the altitude change (with respect to time) $\dot{H}$ referenced to the surrounding air, the speed change (with respect to time) $\dot{V}_{\mathrm{TAS}}$ and the change of aircraft mass $\dot{m}_{\mathrm{AC}}$ corresponding to the aircraft fuel consumption. Note that the gravitational acceleration g is assumed to be constant and its variation with time can be neglected for the calculation of the power imbalance. To convert the power imbalance into an equivalent drag coefficient variation, which is more easy to assess from an engineering point of view, the formulation from [5] is used:

$$\Delta C_{\widetilde{D}} \approx \frac{\dot{E}_{\mathrm{tot,ref}} - \dot{E}_{\mathrm{tot}}}{V_{\mathrm{TAS}} \cdot \overline{q} \cdot S_{\mathrm{Wing}}} \tag{2}$$

This non-dimensional equivalent drag coefficient is calculated by comparison of the current determined power imbalance $\dot{E}_{\mathrm{tot}}$ and a predefined reference value $\dot{E}_{\mathrm{tot,ref}}$. The performance reference value is a function of the aircraft flight state defined by parameters such as altitude, speed and load factor, and also the aircraft configuration (e.g., mass, high lift system configuration) and propulsion system state. If required, some corrections for additional influences, e.g., flight with side slip condition could be applied [5]. Furthermore, the airspeed V_{TAS} is derived from several measurements and contains a combination of aircraft flight path velocity and wind speed (both to be understood as 3D vectors). For the time derivative $\dot{V}_{\mathrm{TAS}}$, the component related to the change of wind vector should be ignored in order to prevent it from falsifying the performance estimate. A variable wind-corrected energy change $\dot{E}_{\mathrm{tot,corr}}$ could then be used changing $\dot{V}_{\mathrm{TAS}}$ in Eq. (1) to $\dot{V}_{\mathrm{TAS},\dot{\vec{V}}_{\mathrm{k}}}$ considering only the airspeed change related to the flight path.

The equivalent drag coefficient is well comparable to a predefined threshold value and indicates an abnormal performance variation when exceeding. This is further independent from the flight point. Note that a drag coefficient value is well interpretable in terms of aerodynamics and flight mechanics by aerospace engineers and allows a direct assessment of the magnitude of aerodynamic degradation caused by icing. Within the IID, this drag coefficient is normalized with the aircraft's zero-lift drag coefficient and compared to a predefined threshold. It has been shown, that this implementation provides some advantages, as it becomes fully independent of the current flight condition and can therefore be used during different flight phases. With the proposed normalization, the threshold can further be defined more independently of the specific aircraft.

The choice for the representation of the performance reference is also dependent on the requirement for adaptation to a specific aircraft. For example, if the performance reference should be adapted over the lifetime of the aircraft to cover the normal long-term "Expectable Variation" of flight performance, a comprehensive multi-dimensional table model would be preferable. In case of SENS4ICE flight test implementation a different approach with separated aerodynamics and engine models is used for pratical reasons (see section 3.2). But the latter would not be suitable for the long-term model adjustment due to its formulation.

Further detailed information on performance-based ice detection, which is already under patent protection in several countries [9], can be found in Ref. [5].

3.1. Implementation of the Indirect Ice Detection Algorithm

The indirect ice detection is implemented as a modular set of functions, including the core detection algorithm, the required data preprocessing and a subsequent detection result filtering to prevent false detections. The latter also guarantees the necessary system robustness against e.g., measurement noise/errors, and consequently reliability. Within SENS4ICE, the indirect ice detection is part of the HIDS and its specific implementation allows the detection of performance degradations and therefore

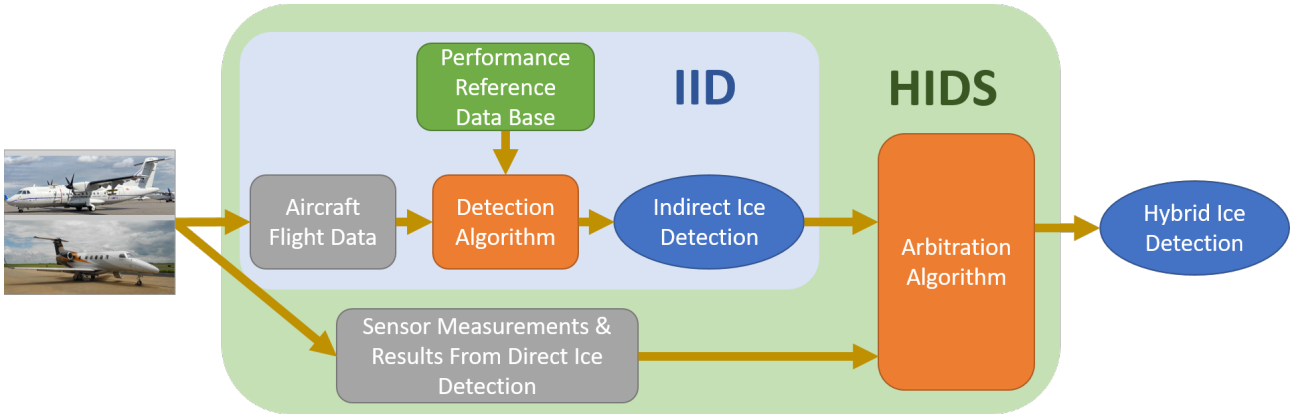

Figure 6 – Visualization of HIDS concept used within SENS4ICE (pictures credit DLR / Embraer / Safire).

the ice accretion (see Fig. 6). The HIDS implementation was designed to be applicable to SENS4ICE flight test campaigns with two highly different aircraft configurations: a light business jet aircraft (Embraer Phenom 300) and a regional class turbo-prop aircraft (ATR 42). This applicability was possible through the generic formulation of the detection methodology itself, not relying on specific information about the aircraft: the required aircraft-specific adaption of the detection was achieved by considering the aircraft-specific reference, which is an input to the algorithm and not part of the core implementation. There are several needs for adjustments inside the IID for a specific aircraft type, mainly as part of the “Aircraft Flight Data” and “Performance Reference Data Base” blocks in Fig. 6:

- flight data preprocessing,
- flight performance reference data base,
- indirect ice detection threshold and confirmation times, and
- detection reliability conditions.

A detailed description about these required adjustments is given in Refs. [6, 21, 22]. The flight performance reference, detection threshold and confirmation times are briefly described below. For the SENS4ICE flight testing, the IID was implemented in MATLAB®/Simulink by DLR and integrated into the HIDS, which was developed by Safran Aerosystems. Hence, it had to be embedded in the corresponding real time software on the dSpace MicroAutoBox for the flight tests.

3.2. Flight Performance Reference Data Base

The IID relies on an accurate flight performance reference, which allows the computed current flight performance to be compared to the measured one within the detection module. A simple way for the definition of the aircraft flight performance reference is the usage of a multi-dimensional table [5, 6]. Another way is to calculate the reference power imbalance from an aerodynamic data base and engine thrust model, if both are available. In such a case, it must be determined if the variation in the reference power imbalance results from changes of the aircraft aerodynamics or the engine performance. For the implementation in SENS4ICE, an engine thrust model was available and the reference power imbalance can be formulated as a function of flight condition, aircraft configurations (using a reference aerodynamic model representation) and the currently predicted engine thrust. Having this separation with an individual aerodynamic reference model, it was possible to adapt the reference aerodynamics to the specific conditions given by the flight test benches having several external probes attached to the test aircraft that influence its flight performance. Also, the performance reference was continuously checked during the flight test campaign to monitor its validity. As presented in Ref. [20], a post-campaign adaption for the Phenom 300 prototype engine thrust reference was required, which could be easily done due to the given separation of aerodynamics and thrust.

Note that this was mainly relevant for the test configuration within the SENS4ICE project and might be different for a potential operational IID implementation in future.
Within the IID implementation, a linear parameter extension of the drag polar representation was already intended, allowing the adaptation of the aircraft aerodynamics to the SENS4ICE aircraft modifications. For a valid result of the IID testing during the icing campaign flights, the new campaign reference for both aircraft was essential. Note that the flight performance reference in SENS4ICE is based on certain a priori knowledge and information obtained from a specific flight data evaluation. But for new aircraft designs it could also be based on the design models and initial prototype flight test results. A detailed description on the flight performance references is given in Refs. [21, 22].

3.3. Detection Threshold, Confirmation Time and Reliability Conditions

A detection threshold on the equivalent drag coefficient is defined to reveal the abnormal flight performance caused by icing. For practical reasons, the detection is not based on the absolute value of the equivalent drag increase, but on a relative value with respect to the zero-lift drag coefficient. In a nominal case, the additional drag coefficient is zero and there is no relative change to the normal drag condition. During normal flight operations there are constant fluctuations of measured flight performance, which have to be considered by the detection algorithm through providing a suitable low-pass filtering function. In addition, the implementation of a confirmation time allows to further prevent false alarms caused by short-time threshold exceedances, if set high enough. The confirmation time is chosen in accordance with the modeling accuracy of the whole IID system chain and quality of flight data, where high quality and accuracy of flight data measurements can lead to relatively short confirmation times and vice versa. For the detection, the confirmation time frame is chosen relatively short to ensure fast response behavior, but for the reset that confirmation time must be much longer to guarantee the threshold is reliably passed and the icing-related performance degradation is not present anymore. For the post-flight evaluation of the IID, the detection threshold was set to 10 % of reference C_{D0} above nominal drag estimation for both campaigns and the confirmation time was fixed at 20 s for the detection with threshold exceeded by more than 50% within the detection window. For resetting, the detection the confirmation time was kept at 180 s.
The IID is designed to run continuously during the whole flight and to monitor the aircraft flight performance and a potential degradation independently from any specific flight phase or maneuver, as discussed in Ref. [5]. The SENS4ICE implementation is experimental and therefore limited to one aircraft specific configuration defined for the flight test in icing conditions. Hence, other aircraft configurations will be detected and the IID is designed to freeze and set an unreliability flag allowing the HIDS to discard the current IID output. A more detailed description is given in Ref. [6].

4. Example from North America flight test campaign

The example flight left St. Louis Regional Airport in Alton, Illinois, on February 25th, 2023, in a north-easterly direction to the great lakes at 11:38 UTC (5:38 local) reaching Eugene F. Kranz Toledo Express Airport in Toledo, Ohio, at 13:42 UTC (7:42 local). Within the vicinity of the great lakes, after around 40 min of flight, icing conditions were found leading to five successful encounters, also including supercooled large droplet icing conditions as defined in App. O. Note that during the encounters the total amount of SLD was small compared to the other supercooled water drops with lower size, as it was expected due to the rarity of SLD in the atmosphere. An overview of the flight is given in Fig. 7 including the flight track and icing encounters.
The following flight test results contain a theoretical ice accretion rate (IAR) for a cylinder with a diameter of $D_{\text{ref}} = 1$ in. It is based on the measurements of the atmospheric conditions (liquid water content LWC, median volumetric droplet diameter MVD) and the aircraft state (true airspeed V_{TAS}):

$$IAR = \frac{\beta_{\text{col}} \cdot LWC \cdot V_{\text{TAS}} \cdot FF}{\rho_{\text{ice}}}, \tag{3}$$

with the corresponding collection efficiency β_{col} being a function of speed, atmospheric condition (MVD, LWC), water ρ_{water} and air density ρ_{air} and air viscosity μ_{air}:

$$\beta_{\text{col}} = f(V_{\text{TAS}}, MVD, LWC, D_{\text{ref}}, \rho_{\text{air}}, \rho_{\text{water}}, \mu_{\text{air}}). \tag{4}$$

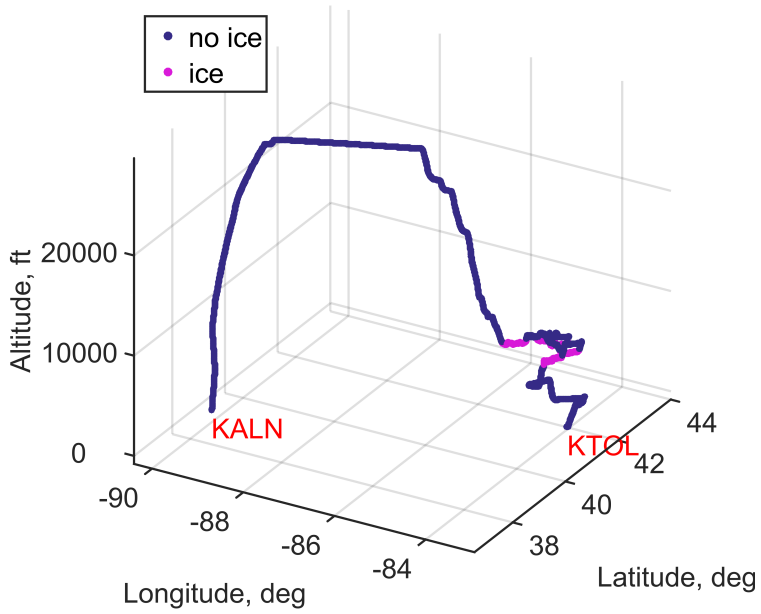

Figure 7 – Flight track from SENS4ICE North America icing campaign flight on February 25rd, 2023 (St. Louis Regional Airport, KALN, to Eugene F. Kranz Toledo Express Airport, KTOL): geodetic position and altitude with indication of icing encountered.

The freezing fraction is a complex function FF influenced by the atmospheric conditions, temperature, heat exchange, flight conditions, etc. calculated for each time sample. A complete outline of the corresponding equations is given in Ref. [23].

4.1. Indirect ice detection system performance during North America campaign flight

The IID performance during this example is evaluated for the five icing encounters at the end of the flight near Toledo, Ohio. These are visualized as time history plots in Fig. 8, which contains the whole flight as overview. Information about the individual encounter can be found in Ref. [22]. The top plot contains the altitude and indicated airspeed in which it is clearly visible that the aircraft was intentionally descending into the (expected) icing conditions, reaching these after approximately 12:20 UTC with reduced airspeed, and climbing again out of these while increasing the airspeed after a certain encounter time. This was repeated four times while deicing the aircraft in between in warmer air above the icing layer with higher airspeed resulting in an sufficiently high total air temperature for the de-icing. Figure 9 shows an example of ice accretion on the outer parts of the right wing of the Phenom 300 prototype during one icing encounter of the SENS4ICE US flight test campaign.

The second plot (from top) shows the nominal drag coefficient estimation (normalized with clean aircraft zero-lift drag) and gives a direct impression about the performance degradation. In parallel the IID detection output is given, allowing a direct comparison of drag increase and IID detection performance. Note that the shown data are results of the replayed IID calculation directly fed with aircraft data/measurements including the post-campaign modified engine model described in [20]. There is no significant difference in the IID code implementation between the desktop replay and the flight test implementation within the HIDS (dSpace box) except for the used/adjusted engine thrust model. The peaks visible in the drag estimation plot result from still existing deficiencies after initial engine model modification, which could be further removed by an additional model update. Nevertheless, for the sake of the results presented, this is not necessary.

The third plot (from top) contains the information about the encountered icing conditions in form of a theoretical ice accretion rate calculated for a 1 in diameter cylinder based on the measured atmospheric conditions. The bottom plot contains the measured static air temperature as well as the averaged engine fan speed (left and right right, assuming symmetric thrust conditions). During the descend into the icing conditions the temperature decreases significantly and increases again

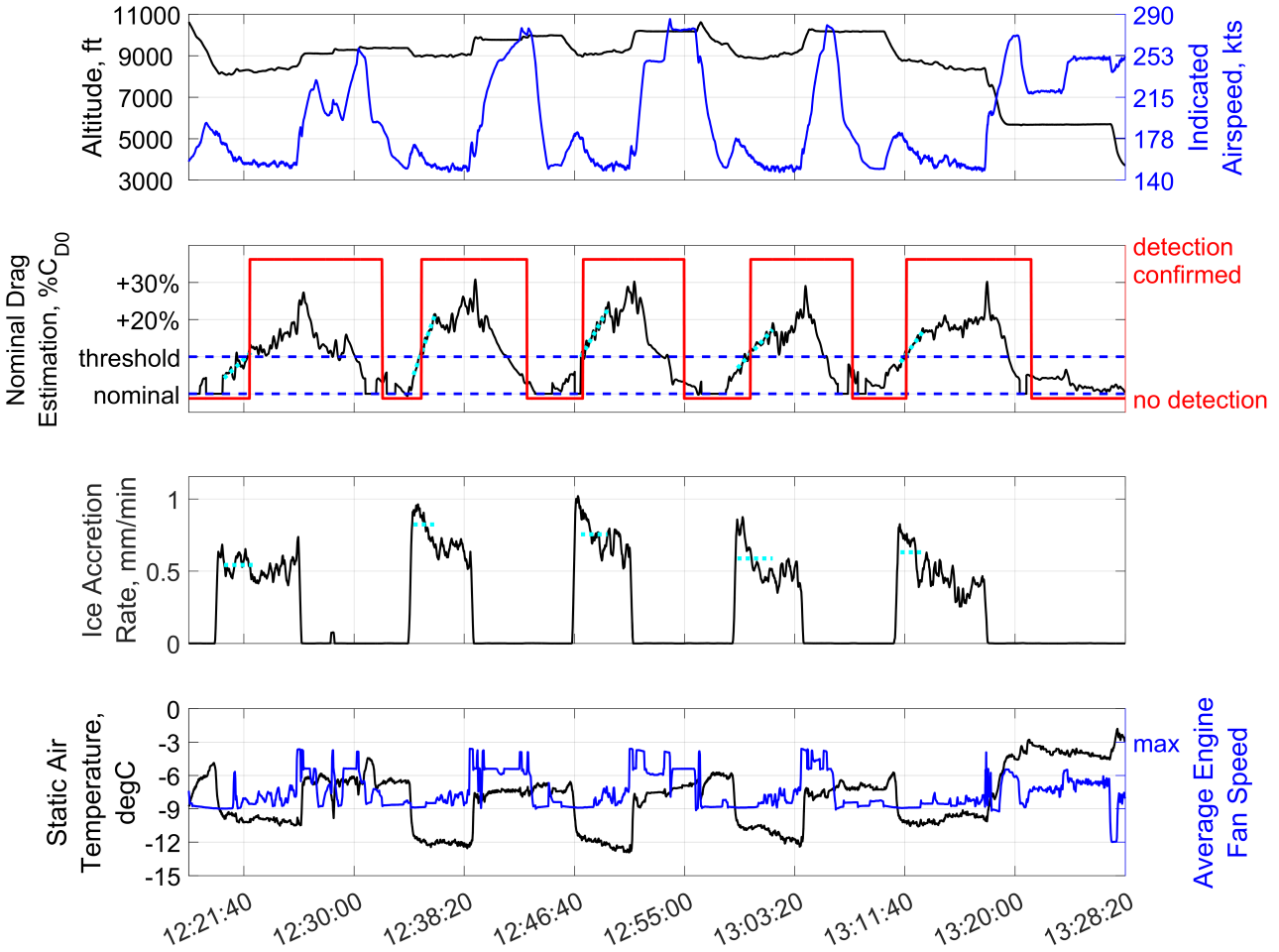

Figure 8 – Time history of IID system performance during example flight on February 25rd, 2023 (12:17:30 UTC to 13:36:40 UTC): altitude and indicated airspeed (top), relative drag coefficient and IID detection output (second plot), and theoretical ice accretion rate based on the encountered icing conditions (third plot), and static air temperature and average engine fan speed (bottom); detection threshold at 10 % above nominal drag estimation and adjusted engine thrust model behavior.

after climbing out of the conditions, indicating an atmospheric inversion layer. This allows a direct assessment about the icing encountered leading to airframe ice accretion and hence a performance degradation, together with the possibility to cross-check the detection reset with the flight through warm air and consequent de-icing. The averaged engine fan speed is directly linked to the total engine thrust and therefore gives an information about the forces applied to the aircraft in combination with the aerodynamic performance degradation.

Note that the second and third plot also include cyan dashed lines indicating a linear regression of the nominal drag increase during the encounter and the corresponding mean values of the ice accretion rate. These will be used to analyze the change of aerodynamics during the encounter presented in section 4.2.

During all encounters of this flight, the IID was able to reliably detect the performance degradation within two minutes or less after the ice build-up started. The confirmed detection remained every time until the aircraft left the conditions and was completely de-iced again. For these encounters, the time to restore the nominal flight performance and to reset the detection flag was approximately the same as the duration during which the aircraft stayed in the conditions itself. This shows the great value of the IID because it reliably indicates the aircraft degradation, being eventually critical for the aircraft operation, even if the icing conditions are already left. This is one of the keys related to the layered safety concept provided by SENS4ICE, including the HIDS approach.

Figure 9 – Example of ice accretion on the Phenom 300 prototype outer right wing and winglet (white, glossy layer) during one flight of the SENS4ICE US icing flight test campaign; with permission, copyright Embraer

4.2. Aerodynamic Degradation due to icing

Figure 10 shows the aircraft drag polar calculated from the measured data for the whole flight (flaps retracted, gear up and no spoiler deflection). For each data point available in the measurement, the lift and drag coefficient is calculated based on the available inertial and inflow measurements as well as the adjusted engine thrust model (see, e.g., Ref. [20]). The plot further contains the aerodynamic reference used for the flight test reflecting the Phenom 300 prototype characteristics with all SENS4ICE modifications (red line). Furthermore, the drag polar data includes an indication of the corresponding IID calculated relative drag (normalized with base aircraft zero-lift drag). Blue marks indicate a nominal drag, which means that there is no increase detected. The more the aircraft is degraded, the more the relative drag increase and the marks are moving to the right getting lighter. Orange marks indicate the maximum calculated drag increase, which has to be taken with caution in the presented cause for, e.g., the still existing minor shortage of engine thrust approximation used. Anyway, the cyan marks show a drag increase of around 25 %, which was the maximum experienced present during the icing encounters as shown in Fig. 8. Knowing that the main degradation is related to an increase of surface friction on (mainly) unprotected aircraft parts, this is reasonable. This is also well comparable to the results for App. C conditions presented in Ref. [20].

The herein presented flight 1476 contains five different App. O icing encounters with a significant amount of supercooled large droplets. With the fundamental knowledge and scientific background on SLD ice accretion, the expectation on the degradation from these SLD encounters was to be significantly worse or more critical than the degradation from the App. C icing encounters. But, a direct comparison with the results from the previous icing flight 1475, presented in Ref. [20], does not directly reveal a difference in the aerodynamics degradation, see Fig. 11. Both flights show a noticeable aerodynamic degradation due to ice accretion on the airframe, but the expected significant differences of the degradation between App. C and App. O are not visible at the first glance. Nevertheless, this does not reduce the criticality of SLD-ice impact on aircraft aerodynamics in any way, but shows the overall degrading influence is significantly related to the icing conditions encountered. It is very important to state again that SLD-ice can produce very critical ice shapes on the airframe and was cause to various catastrophic accidents in the past. Here it shows that further analysis is required to reveal this criticality, which is not easily visible in the aircraft drag polar results.

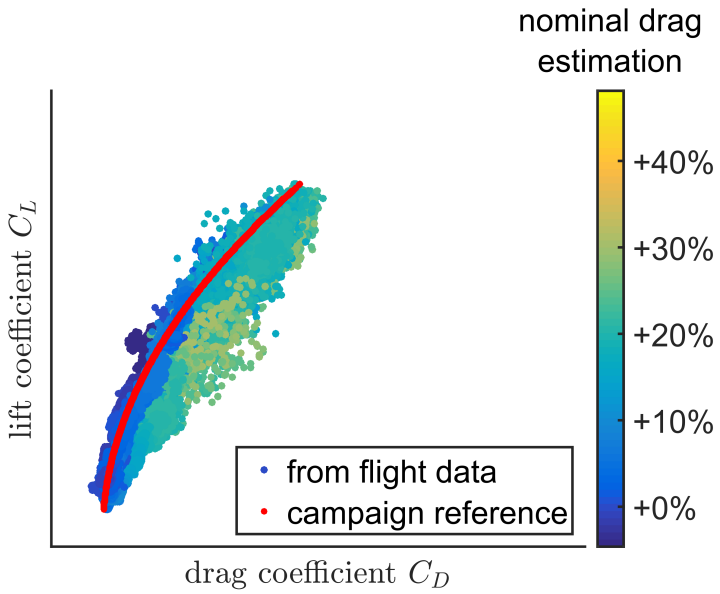

Figure 10 – Aircraft drag polar from example flight (after engine thrust model adjustment): calculated lift and drag coefficient from flight data measurements and reference for the Phenom 300 prototype with SENS4ICE modifications; drag coefficient data including the indication of relative drag calculated by IID with adjusted engine thrust during data replay.

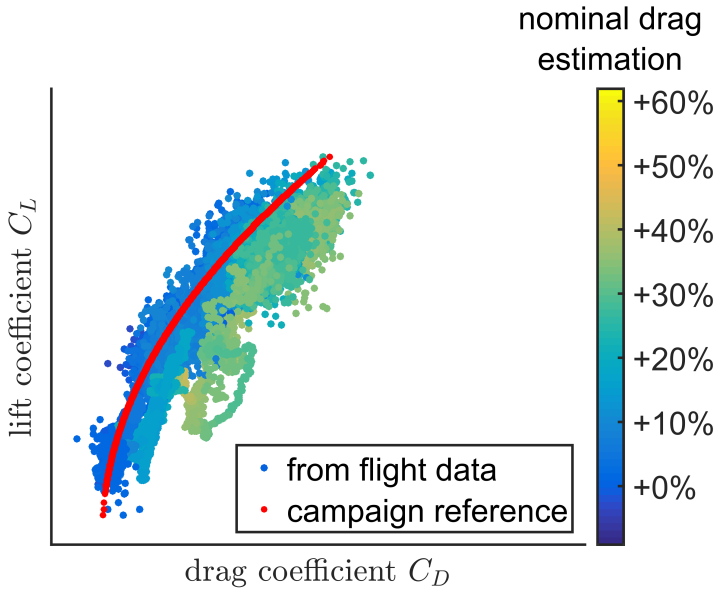

Figure 11 – Aircraft drag polar from previous icing flight 1475 (after engine thrust model adjustment): calculated lift and drag coefficient from flight data measurements and reference for the Phenom 300 prototype with SENS4ICE modifications; drag coefficient data including the indication of relative drag calculated by IID with adjusted engine thrust during data replay.

Figure 8 contains the linear regression of the nominal drag estimation (increasing drag) during the encounters. The corresponding slope is an approximation of the time derivative $\frac{\partial C_D}{\partial s}$ during the performance degradation. Using the mean ice accretion rate also indicated in Fig. 8 allows correlating the drag change to the build-up of ice on the airframe. For the given encounters, the main aerodynamic degradation is related to the increase of surface roughness caused by the ice accretion on the unprotected airframe surfaces. It is assumed, that the SLD-icing conditions have a significantly different impact on the surface roughness than the “classical” App. C condition and hence a different effect on the drag change [24].
The results are given in Fig. 12 as drag coefficient change $\frac{\partial C_D}{\partial s}$ over theoretical ice accretion rate for the five App. O encounter. In addition, the corresponding results of the remaining App. C encounters for the US campaign are plotted for comparison. It is clearly visible, that the ice formations related to App. O conditions cause higher rates of drag coefficient change than the comparable App. C conditions at equivalent accretion rates. For similar influence on the aircraft drag, significantly higher ice accretion rates in App. C conditions are required. This result agrees well with the expectations on the influence of SLD-ice on the aircraft characteristics. Nevertheless, one has to keep in mind, that the available data is limited and there are also some App. O points at higher IAR with relatively low drag impact. Hence, the findings from this evaluation do only allow general conclusions given the limited number of observations.

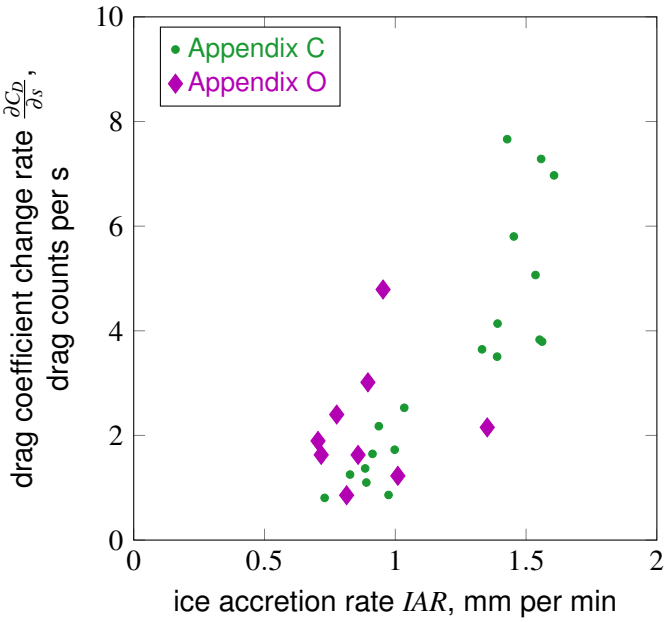

Figure 12 – Overview of drag coefficient change vs. theoretical ice accretion rate for different icing encounters; App. C and App. O conditions from US campaign flights.

5. Example from the European flight test campaign

Results from one specific flight of the European icing flight test campaign are presented briefly. More detailed results and evaluations of the European campaign flights can be found in Refs. [21, 22]. During the presented flight, different icing conditions, including classical App. C and the rare SLD conditions (App. O), were successfully encountered on April 24th, 2023 in Southern France. Note that for safety reasons, the mechanical de-icing system of the ATR42, i.e. pneumatic boots, was activated during the encounters according to the given operational requirements, which lead mainly to intercycle ice shapes on the wing's and horizontal tail's leading edges. Figure 13 contains an overview of the flight track from the flight around the CERs Marsan and Cazaux west of Toulouse. It can be clearly seen, that during the flight icing was encountered at a specific altitude and after a certain time, the aircraft descended to perform a full airframe de-icing in warmer air.

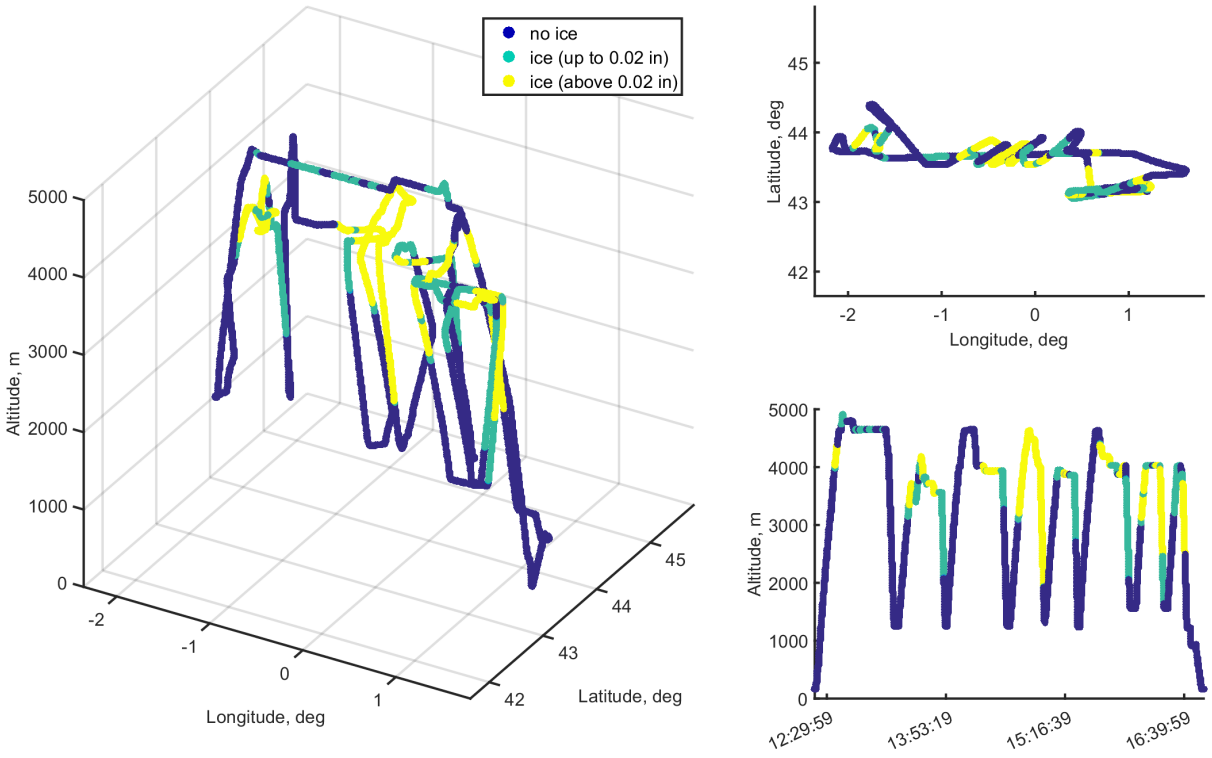

Figure 13 – Flight track from SENS4ICE European icing campaign flight on April 24th, 2023 around Toulouse/Marsan/Cazaux: geodetic position and altitude with indication of icing encountered / build-up.

5.1. Indirect ice detection system performance during European campaign flight

A time history of the IID detection behavior during this specific flight is given in Fig. 14. The four different plots contain: altitude and indicated airspeed (top), nominal drag estimation and IID detection output (second plot), ice build-up on aircraft ice accretion sensor and static air temperature (third plot), the theoretical ice accretion rate for a 1 in diameter cylinder (fourth plot) and MVD and LWC of encountered icing conditions (solid line) including the indication of the amount of SLD (dashed lines) (bottom). It is clearly visible that the major icing events / encounter led to a confirmed detection of abnormal flight performance by the indirect ice detection.

During the flights with the Safire ATR42, images of the inner left and right wing leading edges as well as the horizontal tail were recorded with specifically mounted cameras looking out of certain windows. The images allow a post-flight evaluation of the icing condition as the estimated aircraft

flight performance can be correlated with the actual ice accretion[1]. Figure 15 shows a specific view on the leading edges of the left and right wing (from below) together with the horizontal tail for different times during the third major icing encounter of the presented flight between 14:18 UTC and 14:37 UTC (see Fig. 14). At 14:19:25 UTC, when the encounter started, the airframe was free of visible ice accretion. But around two minutes later and a confirmed IID detection information, the airframe shows an icing layer which is already broken on the wing leading edges by the active de-icing system. During the next minutes, the formation does not change in total and although the boots remove some ice, new formations build-up, which then cause almost no change in the estimated drag resulting from the IID (more than 50 % above nominal). It is interesting to see that at around 14:29 UTC, when large drops were encountered, the wings seem to have less ice accretion then before – resulting in the reduction of the additional drag estimated by the IID between 14:29 UTC and 14:31 UTC – because of a presumably good effectivity of the ice protection system. The drag rises again briefly after, where a glaze ice formation is visible on the aircraft (14:32:37 UTC in Fig. 15), which is presumably a result of the ongoing SLD icing situation. Anyway, this result shows that a currently present ice encounter might not have an immediately noticeable adverse effect on the aircraft aerodynamics. Monitoring just the icing conditions might consequently not give a correct indication on the criticality of the encounter, even if the situation looks dangerous in terms of water drops in the air. But the continuous monitoring of the ice formation and corresponding aerodynamics degradation will give the comprehensive view on the current situation required for a safe aircraft operation. After descending and passing through the 0 degC temperature layer, the aircraft got free of ice again (14:36 UTC).

[1] Note that these images were thankfully released by Safire for publication, which is a great advantage for the public documentation of the European flight test campaign. Similar images from the US campaign are not publicly available through Embraer IP protection restrictions.

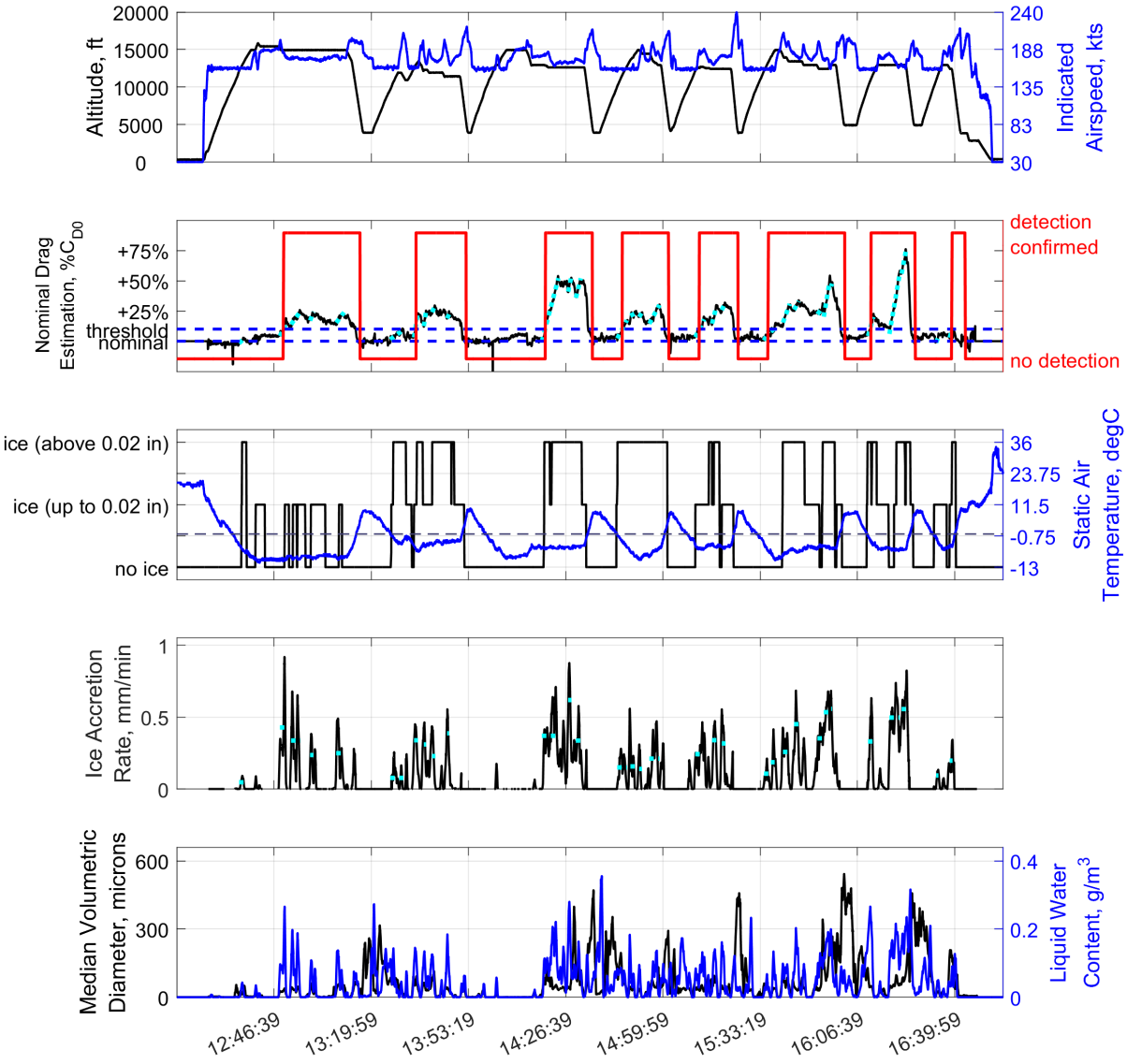

Figure 14 – Time history of IID system performance during the example flight on April 24th, 2023 (12:13 UTC to 16:56 UTC): altitude and indicated airspeed (top), nominal drag estimation and IID detection output (second plot), ice build-up on aircraft ice accretion sensor and static air temperature (dashed line 0 degC) (third plot), theoretical ice accretion rate (fourth plot), and MVD and LWC of encountered icing conditions (solid line) including the indication of the amount of SLD (dashed lines) (bottom); detection threshold at 10 % above nominal drag estimation.

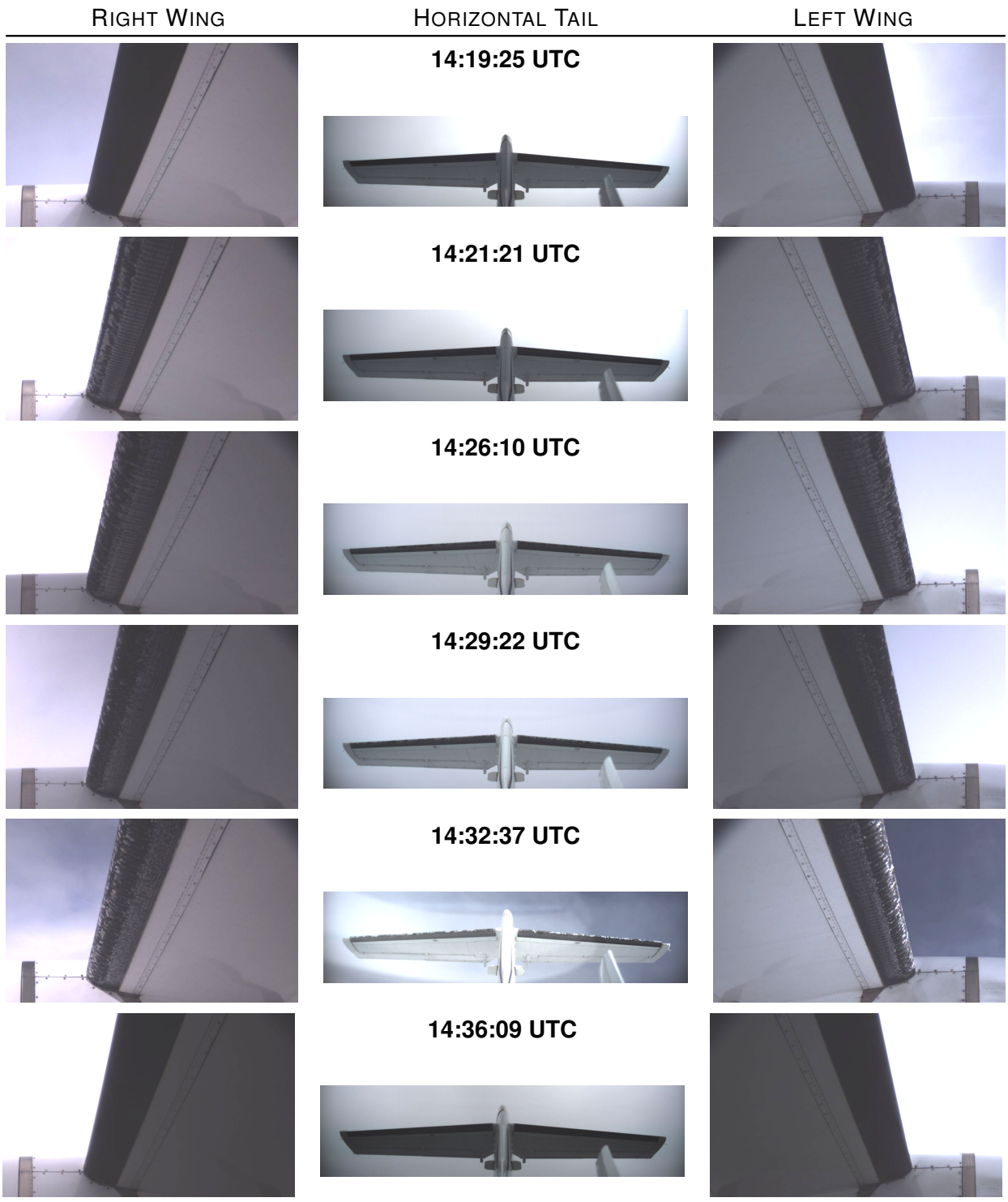

Figure 15 – Evolution of ice accretion on the airframe during icing encounter: camera views on left & right wing and horizontal tail for specific moments during flight (increased brightness and contrast); corresponding to encounter and IID detection given in Fig. 14 between 14:18 UTC and 14:37 UTC; credit Safire / SENS4ICE project.

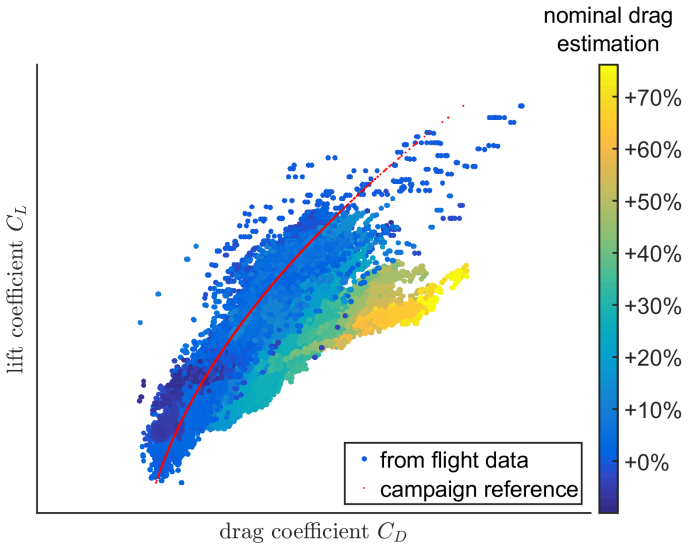

Figure 16 – Aircraft drag polar from example flight on April 24th, 2023: calculated lift and drag coefficient from flight data measurements and reference for the Safire ATR 42-320 with SENS4ICE modifications; drag coefficient data including the indication of nominal drag estimation calculated by IID.

5.2. Aerodynamic degradation due to icing

Figure 16 shows the aircraft lift and drag data (drag polar) calculated from the measured data for the whole flight (flaps retracted, gear up). For each data point available in the measurement, the lift and drag coefficient is calculated based on the available inertial and inflow measurements as well as the given engine thrust. The plot contains the aerodynamic reference used for the flight test reflecting the Safire ATR 42 characteristics with all SENS4ICE aircraft modifications (red line). The maximum degradation (large drag coefficients at medium lift coefficients, yellow and orange points) is correlated with a nominal drag estimation change of around 70 % (as given in the color bar on the right), but having 30 % to 40 % change in average (cyan points) related to icing in a more continuous manner, meaning that the degradation is kind of saturated. This is also visible in the time history plots from this flight. Knowing that the main degradation is related to an increase of surface friction on (mainly) unprotected aircraft parts, this is reasonable. Similar to the results of the drag coefficient change for the Phenom 300 flight test aircraft during the icing encounters of the US flight test campaign (see section 4.1), the obtained data from the European campaign was analyzed accordingly for the Safire ATR42. Again, the slope of the drag change serves as an approximation of the time derivative $\frac{\partial C_D}{\partial s}$ during the performance degradation (ice build-up) and the mean ice accretion rate is calculated from the corresponding flight data, as given in Fig. 14. Figure 17 contains these results as drag coefficient change $\frac{\partial C_D}{\partial s}$ over theoretical ice accretion rate for different icing encounters, also including data from other flights of the European campaign. For this, only significant data sets with encounters lasting over 100 s were selected. During the European flight test campaign, the icing encounters were not as distinct as during the US campaign, where it was possible to enter stratiform clouds with constant icing conditions for precisely determined timespans. In contrast, in April 2023 these conditions where not present around southern France and the icing encounters where mainly driven by incoming fronts from the Atlantic ocean with varying conditions in smaller clouds. To not bias the results with data from very short encounters, for the first evaluation only longer encounters where selected for the analysis presented herein. In Fig. 17, it is distinguished between encounters that lasted more than 100 s, but were shorter than 200 s, and ones that were over 200 s long. This further helps to analyze the different effects of icing encounters with different times. The results are well comparable to the results presented in Fig. 12 for data from the US flight test campaign, and generally lead to a similar finding: ice formations related to App. O conditions cause in general higher rates of drag coefficient change than the comparable App. C conditions at same accretion rates. For similar influence on the aircraft drag, significantly higher ice accretion rates in App. C conditions are required.

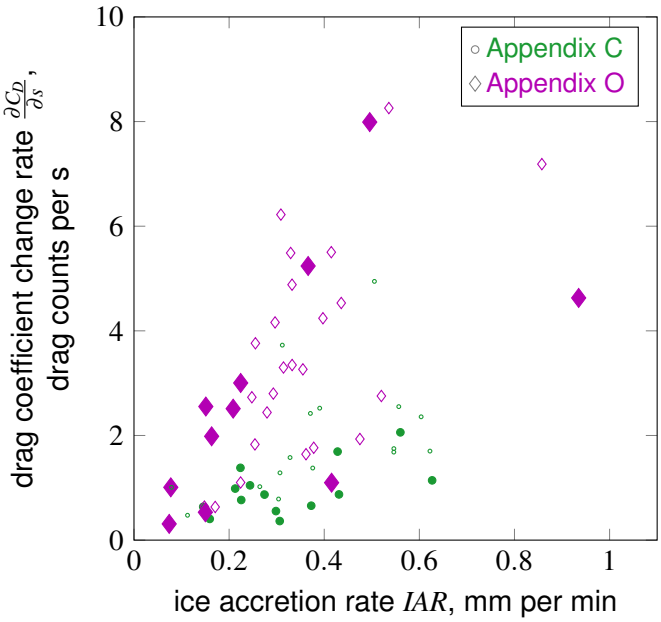

Figure 17 – Overview of drag coefficient change vs. theoretical ice accretion rate for different icing encounters; App. C and App. O conditions from European campaign flights; filled marks indicating encounter times above 200 s and small empty marks correspond to encounter times between 100 and 200 s.

6. Summary and Conclusions

The SENS4ICE project is a big step towards successful and reliable detection of different icing conditions including SLD (Appendix O conditions). One key to achieve this goal is the indirect ice detection system based on aircraft performance degradation, which provides several advantages compared to direct detection (ice sensors), which are mainly complementary: direct sensors allow to detect the atmospheric conditions prone to icing whereas the indirect detection gives information about the icing effects on the aircraft. The IID provides e.g., retrofit capabilities, a simple software solution and highly beneficial information about the remaining aircraft capabilities for safe aircraft operations. In addition, the indirect ice detection represents a second pillar for ice detection redundancy when hybridized and hence reduces the risk for common cause failures. It is based on the reliable measurements of the aircraft flight condition normally available in modern aircraft avionics.

The IID showed very good performance during both flight test campaigns. The IID was well capable to detect the icing-related performance degradation and reliably monitor the corresponding drag increase. In addition, further modification made on the IID post-flight significantly enhanced the system performance by detecting flight performance degradations in a more sensitive and robust way. Nevertheless, the current version of the IID is an experimental system tailored to the specific flight test benches and their configurations during the SENS4ICE flight test campaigns (TRL 5 after flight test campaign within the HIDS implementation). For an operational use within an in-service aircraft fleet, the algorithm must be further enhanced and implemented into the aircraft avionics, which was clearly not the scope of SENS4ICE. Although other direct ice measuring approaches for the detection of icing conditions or ice accretion on the airframe could deliver a partly similar information, the indirect detection using the performance monitoring approach would not require modifications of existing and future aircraft.

The prototype running during the flight test campaigns was already designed to be highly adaptive to “known” changes of the aircraft flight performance. The modification to the specific flight test bench prior to the flight test has proven the designed system flexibility. Hence, the system seems highly applicable to other transport aircraft or even any fixed-wing aircraft design with reasonable effort. In addition, it will be possible to use the information about the nominal flight performance during aircraft design on the manufacturer side together with expectations on the aerodynamic degradation caused by icing to define the specific implementation of the IID, including it in the ice protection system defini-

tion. During the SENS4ICE project, this process was sketched as no specifically detailed information about the icing impact on both flight test benches was available, but the IID showed very good results during the flight test. This verifies the approach.
Especially for smaller aircraft not equipped with direct ice detection technologies, the IID can be a valuable option for ice detection as a standalone system. In addition, the system might give a high potential for monitoring the aircraft icing status in terms of present ice accretion degrading the flight characteristics and the effectiveness of countermeasures (anti-ice and de-icing systems) trying to prevent any negative impact of icing on the aircraft operations, both for a standalone system or as part of the hybrid approach. Such an evaluation might be possible with the data available from SENS4ICE flight test, but was not in the specific scope of the project.

Concluding on the SENS4ICE project results, the following can be stated related to the performance-based ice detection also with regard to further research needs:

- SENS4ICE contributed to the enhancement of aviation icing safety by the development of the revolutionary hybrid approach including novel detection technologies for the rare SLD conditions. Further development to robustly and reliably classify safety relevant icing conditions (e.g. freezing drizzle/rain) and a definition of a clear path for certification requirements for sensor technologies (including software algorithms) is needed.
- SENS4ICE showed that safe aircraft operation in icing conditions are related not solely to atmospheric icing conditions but also ice formation on airframe and degradation of flight characteristics. The impact of SLD icing in App. O must always be considered by effect on aircraft (relevant for certification) and not only detection of icing conditions. This requires a change of view on certification path and/or definition acceptable means of compliance particularly for new aircraft designs.

7. Contact Author Email Address

christoph.deiler@dlr.de

Disclaimer

The Phenom 300 flight test data analyzed is based on an experimental prototype. This aircraft prototype has embedded additional flight test instrumentation and features that do not represent any certified Phenom 300 aircraft model. Therefore, the analysis and performance estimations assessed in this study and within the SENS4ICE project do not represent the Phenom 300's certified performance.

Acknowledgments

The author wants to specially thank his colleague Falk Sachs for the contribution to this work of the IID development and flight test conduction. Within SENS4ICE the hybrid ice detection system was designed and developed by SAFRAN. Without this, the test of the IID during flight would not have been possible. The author wants to especially thank Annagrazia Orazzo and Bruno Thillays for their effort and support on the HIDS software development and hardware implementation on the flight test platforms. The author wants to further thank the SENS4ICE North America campaign flight test team for its structured and professional work to conduct the flight tests, especially Daniel Martins da Silva for coordinating with the SENS4ICE project group. In addition, the author wants to specially thank the SENS4ICE European campaign flight test team for its structured and professional work to conduct the flight tests even on very short notice according to the weather forecasts. A special thank goes to Tetyana Jiang (Safire) for the support with the flight test instrumentation, flight data and in-flight camera footage, and Jean-Philippe Desbios (Safire) for the campaign coordination.
Airborne data was obtained using the aircraft managed by Safire, the French facility for airborne research, an infrastructure of the French National Center for Scientific Research (CNRS), Météo-France and the French National Center for Space Studies (CNES). Distributed data are processed by Safire.

Funding Information

The “SENSors and certifiable hybrid architectures for safer aviation in ICing Environment” (SENS4ICE) project has received funding from the European Union’s Horizon 2020 research and innovation programme under grant agreement N° 824253.

Copyright Statement

References

[1] Steven D. Green. A study of U. S. inflight icing accidents and incidents, 1978 to 2002. Number AIAA 2006-82, Reno, Nevada, USA, January 9th - 12th, 2006. 44th AIAA Aerospace Sciences Meeting and Exhibit, American Institute of Aeronautics and Astronautics, Inc. (AIAA). DOI: 10.2514/6.2006-82.

[2] Steven D. Green. The icemaster database and an analysis of aircraft aerodynamic icing accidents and incidents. Technical Report DOT/FAA/TC-14/44, R1, Federal Aviation Administration, Atlantic City, NJ, USA, Oct. 2015.

[3] Anon. *Final Report (BFU 5X011-0/98)*. German Federal Bureau of Aircraft Accident Investigation, Braunschweig, Germany, April 2001.

[4] Anon. *Aircraft Accident Report (NTSB/AAR-96/01, DCA95MA001), Safety Board Report*. National Transportation Safety Board (NTSB), Washington, DC, USA, July 9th 1996.

[5] Christoph Deiler and Nicolas Fezans. Performance-based ice detection methodology. *Journal of Aircraft*, 57(2):209–223, March 2020. DOI: 10.2514/1.C034828.

[6] Christoph Deiler and Falk Sachs. Design and testing of an indirect ice detection methodology. Vienna, Austria, June 20th - 22nd 2023. SAE International Conference on Icing of Aircraft, Engines, and Structures, SAE International, Paper 2023-01-1493. DOI: 10.4271/2023-01-1493.

[7] Carsten W. Schwarz. The SENS4ICE EU project – sensors and certifiable hybrid architectures for safer aviation in icing environment – project overview and initial results. Stockholm, Sweden, September 4th - 9th 2022. 33th Congress of the International Council of the Aeronautical Sciences (ICAS). `https://icas.org/ICAS_ARCHIVE/ICAS2020/data/papers/ICAS2022_0794_paper.pdf`.

[8] Carsten W. Schwarz. SENS4ICE EU project preliminary results. Vienna, Austria, June 20th - 22nd 2023. SAE International Conference on Icing of Aircraft, Engines, and Structures, SAE International, Paper 2023-01-1496. DOI: 10.4271/2023-01-1493.

[9] Christoph Deiler and Nicolas Fezans. Method and assistance system for detecting a degradation of flight performance, 2017. Patent Numbers: US11401044B2, EP3479181B1, WO2018002148A1, FR3053460B1, CA3029467A1, ES2919573T3.

[10] Tina Jurkat-Witschas, Johannes Lucke, Carsten W. Schwarz, Christoph Deiler, Falk Sachs, Simon Kirschler, Deniz Menekay, Christiane Voigt, Ben Bernstein, Olivier Jaron, Frank Kalinka, Alessandra Zollo, Lyle Lilie, Johanna Mayer, Christian Page, Benoit Vié, Aurelien Bourdon, Rogerio Pereira Lima, and Luiz Vieira. Overview of cloud microphysical measurements during the SENS4ICE airborne test campaigns: Contrasting icing frequencies from climatological data to first results from airborne observations. Vienna, Austria, June 20th - 22nd 2023. SAE International Conference on Icing of Aircraft, Engines, and Structures, SAE International, Paper 2023-01-1491. DOI: 10.4271/2023-01-1491.

[11] Anon. Ice accretion simulation. AGARD Advisory Report 344, Advisory Group for Aerospace Research & Development (AGARD) - Fluid Dynamics Panel Working Group 20, North Atlantic Treaty Organization (NATO), Neuilly-Sur-Seine, France, December 1997.

[12] Michael B. Bragg, William R. Perkins, Nadine B. Sarter, Tamer Başar, Petros G. Voulgaris, Holly M. Gurbacki, James W. Melody, and Scott A. McCray. An interdisciplinary approach to inflight aircraft icing safety. Number AIAA 98-0095, Reno, Nevada, USA, January 12th-15th 1998. 36th AIAA Aerospace Sciences Meeting and Exhibit, American Institute of Aeronautics and Astronautics, Inc. (AIAA). DOI: 10.2514/6.1998-95.

[13] Thomas T. Myers, David H. Klyde, and Raymond E. Magdaleno. The dynamic icing detection system (dids). Reno, Nevada, USA, January 10th - 13th, 1999. 38th AIAA Aerospace Sciences Meeting and Exhibit, American Institute of Aeronautics and Astronautics, Inc. (AIAA). DOI: 10.2514/6.2000-364.

[14] James W. Melody, Tamer Başar, William R. Perkins, and Petros G. Voulgaris. Parameter identification for inflight detection and characterization of aircraft icing. *Control Engineering Practice*, 8(9):985–1001, September 2000. DOI: 10.1016/S0967-0661(00)00046-0.

[15] Michael B. Bragg, Tamer Başar, William R. Perkins, Michael S. Selig, Petros G. Voulgaris, James W. Melody, and Nadine B. Sater. Smart icing systems for aircraft icing safety. Reno, Nevada, USA, January 14th - 17th 2002. 40th AIAA Aerospace Sciences Meeting and Exhibit, American Institute of Aeronautics and Astronautics, Inc. (AIAA). DOI: 10.2514/6.2002-813.

[16] Rahmi Aykan, Chingiz Hajiyev, and Fikret Caliskan. Aircraft icing detection, identification and reconfigurable control based on kalman filtering and neural networks. San Francisco, California, USA, August 15th - 18th 2005. AIAA Atmospheric Flight Mechanics Conference and Exhibit, American Institute of Aeronautics and Astronautics, Inc. (AIAA). DOI: 10.2514/6.2005-6220.

[17] David R. Gingras, Billy P. Barnhart, Richard J. Ranuado, Thomas P. Ratvasky, and Eugene A. Morelli. Envelope protection for in-flight ice contamination. Orlando, Florida, USA, January 5th - 8th, 2009. 47th Aerospace Sciences Meeting, American Institute of Aeronautics and Astronautics, Inc. (AIAA). DOI: 10.2514/6.2009-1458.

[18] Christoph Deiler. Evaluation of aircraft performance variation during daily flight operations. Friedrichshafen, Germany, Sept. 2018. Deutscher Luft- und Raumfahrtkongress, Deutsche Gesellschaft fur Luft- und Raumfahrt (DGLR). DOI: 10.25967/480025.

[19] Christoph Deiler. Aerodynamic model adjustment for an accurate flight performance representation using a large operational flight data base. *CEAS Aeronautical Journal*, 14(2):527–538, Mar. 2023. DOI: 10.1007/s13272-023-00659-w.

[20] Christoph Deiler. Testing of an indirect ice detection methodology in the Horizon2020 project SENS4ICE. Stuttgart, Germany, September 19th-21st 2023. Deutscher Luft- und Raumfahrtkongress, Deutsche Gesellschaft für Luft- und Raumfahrt (DGLR). https://elib.dlr.de/197520/.

[21] Christoph Deiler. Performance-based ice detection first results from SENS4ICE european flight test campaign. Orlando, Florida, USA, January 8th - 12th 2024. AIAA Scitech Forum, American Institute of Aeronautics and Astronautics, Inc. (AIAA). DOI: 10.2514/6.2024-2817.

[22] Christoph Deiler. Evaluation of the indirect ice detection system performance during the SENS4ICE flight test campaigns. Bristol, UK, June 11th - 13th 2024. CEAS Conference on Guidance, Navigation and Control (EuroGNC), Paper CEAS-GNC-2024-002. https://eurognc.ceas.org/archive/EuroGNC2024/pdf/CEAS-GNC-2024-002.pdf.

[23] EUROCAE ED 103. *Minimum Operational Performance Standard For Inflight Icing Detection Systems, Revision B*. European Organization for Civil Aviation Equipment, 9 – 23 rue Paul Lafargue, 93200 Saint-Denis, France, Apr. 2022.

[24] Michael Papadakis, Reuben Chandrasekharan, Mike Hinson, Hsiung Wei Yeong, and Thomas P. Ratvasky. Effects of roughness on the aerodynamic performance of a business jet tail. Reno, Nevada, USA, January 14th - 17th 2002. 40th AIAA Aerospace Sciences Meeting and Exhibit„ American Institute of Aeronautics and Astronautics, Inc. (AIAA). DOI: 10.2514/6.2002-242.